Facultad de Ciencias
Universidad de La Laguna

Final Degree Project Report:
Study of the effect of the spatial distribution of wind farms on the variability of the energy produced on island with complex orography

Academictutors: Albano José González Fernández
Judit Carrillo Pérez

Paola Serrano Alemán

1. ABSTRACT

Wind energy is actually a mature technology and can present a functional way to supply the demand of a territory. This resource is not controllable and causes undesired fluctuations in the power system. In order to try to prevent this effect, making it compatible with the highest possible generated power, we have proposed the calculation of the optimal distribution of wind farms by using a Multi-Objective Optimization. The selected territory was the island of Gran Canaria, the third largest island of the Canarian Archipelago, in Spain. The island presents a background with renewable energies, specially wind power, which represents to the highest percentage of green energy produced in this territory. The proposed optimization was applied to the extractable wind power simulations from 1995 to 2004 in the archipelago. Two different cases have been analyzed, one where this island is divided in three different regions and the other into 43 different small areas. For both cases, we have obtained the effective distribution of wind farms that results in a more stable power system.

2. ACKNOWLEDGEMENT

To my father for giving me the excitement to learn, to my mother for giving me the strength to go on, to Adal for his company in the bad times. To my friends for understanding me and to Albano and Judith for trusting me and teaching me that I am capable of things I did not know I was capable of.

Also to the scientific community, especially the women scientists, and all the scientists of the papers referenced in the study, thank you for putting the pieces for the future generations.

CONTENTS

3. INTRODUCTION

In the Canary archipelago there are two things that are never missing whatever the season, the sun and the wind. The former is the main reference of the islands due to its subtropical climate and the latter is thanks to the presence of the trade winds that contribute to the good weather characteristic of the islands. In other words, geographically speaking, the Canary Islands are almost permanently in the ideal conditions to be a good territory for the development and the study of renewable productions.

Moreover, a study by the University of La Laguna [1] has determined that renewable energy has an important and positive effect in the psychosocial progress of the Canarian community. Green energy not only contributes to provide new employment opportunities, but also creates a common consciousness to reduce CO2 emissions in the islands. [2].

Large projects have been carried out on the islands, the most outstanding being the Gorona Del Viento hydroelectric power plant [3] located on the island of El Hierro, whose mission is the self-sustainability of the island by using wind and hydraulic energy, and which is considered today an example for power plants around the world and the significance of the good use of renewable energies in the island territories.

At present, the weight of renewable energy continues growing, and in 2022 it covered almost 20% of the islands' energy demand, being wind energy the largest contributor , with a total of 16.2% to the energy mix of the islands[4] .

In addition, the wind energy is the most mature renewable energy technology of the islands. The archipelago has a total of 524 wind turbines, more than half of which, a total of 273, are located on the island of Gran Canaria[7], being the southeast the area with the highest concentration of wind farms, where the first wind turbine in the province of Las Palmas was installed in 1991 in the area of Arinaga, Agüimes.

The present study has been developed for Gran Canaria, one of the islands of the archipelago, which is characterized by having areas with strong and persistent wind during the summer seasons and less frequent in winter. In general, due to the complex topography of the island, when one area experiences a calm wind, other areas may present higher wind speeds. The wind power, therefore, will depend on how

the wind farms are distributed on the island.

We anticipate that in the study we have suggested a methodology to answer a specific question, is it possible to obtain a distribution of wind farms that guarantee the maximum wind power and also, the minimum variability or standard deviation? Or a distribution where we can choose what magnitude we want to prioritize and how the other changes? Therefore, following this question of getting a spatial distribution, we propose the use of a multi-objective optimization using the genetic algorithm NSGA-II[8].

The Non-dominated Sorting Genetic Algorithm (NSGA-II) is the most powerful and well-known version of the multi-objective genetic algorithms. It is a fast and very efficient multi-objective evolutionary algorithm, which incorporates the features of an elitist archive and a rule for adaptation assignment that takes into account both the rank and the distance of each solution from the others [9].

To perform the analysis two strategies have been followed. On the one hand, the contribution of small areas, 43, defined by the spatial resolution of the meteorological data, has been studied. On the other, these regions were clustered according to their similarity of temporal wind characteristics.

Thus, the study proposes a method on the most efficient way to locate wind turbines so that future managers can choose their priority between total power or variability or standard deviation, in a quite visual way, as we will see in the following sections.

The document is organized as follows: Section 3 describes the territory under study and the data used. Also the result of the clustering methods to identify the different regions to study, for the first case, is presented. Section 4, focuses on the methodology for the minimization and maximization of the different magnitudes. In Section 5, the result of the methodology is discussed through comparison with the wind farm already installed in the areas. Finally, the conclusions are drawn in section 6.

4. STUDY AREA AND DATA

4.1 Territory

The Canary archipelago is located in the southwest of Spain, about 1,700 kilometers from the mainland, next to the coast of Africa and surrounded by the Atlantic Ocean. Due to the distance of the islands from the Iberian Peninsula, there has always been a need and a quest to obtain energy autonomously in the archipelago. This explains how over the years the islands have been looking for investment in renewable energies as a way to meet the existing energy demand.

Gran Canaria is the territory chosen for the study. This island stands out for being one of the capital islands belonging to the province of Las Palmas, together with Lanzarote, Fuerteventura and La Graciosa.

Figure 4.1: IDECanarias. Protected areas of Gran Canaria

The island has a rounded shape with an extension of almost 1,560 Km^2, and it is the third island of the archipelago with the largest surface. Also, it is the third highest island, with the highest altitude at 1956 m above sea level[5].

We can differentiate the island into two zones. The northeast (Neocanaria) of more recent formation, characterized by terraces and volcanic cones, also some plains, and the southwest (Tamaran), is the oldest area of the island and is noted for the presence of ravines and massifs. In addition, we must emphasize that the island has a total of 32 protected natural[6] areas (see Figure 4.1), which represent 46% of the island's surface area[5].

As we mentioned at the beginning, in the islands there has always been a need to search for energy, due to the great distance between them and the mainland, either by conventional processes, such as the existing power plants that were the first to be installed, or by renewable energies that have been increasing in number during the last few years.

In Gran Canaria, the greatest electrical renewable power obtained is due to wind energy, with 77%, followed by photovoltaic, 21%, and finally biogas, the remaining 2.% [7]. As we can see, wind production is the pillar of the island, this is due to the climate, characterized by an almost steady wind, stronger during the summer months and weaker during the winter.

Figure 4.2: IDECanarias. Wind farms in Gran Canaria.

Even so, not all of the island of Gran Canaria presents the same scenario for the implementation of

this type of facility. The areas with the highest density of farms are located in the southeast of the island, in the municipalities of Ingenio, Agüimes, Santa Lucia de Tirajana and San Bartolomé de Tirajana. We can also highlight the northwest area with the municipalities of La Aldea de San Nicolas, Agaete and Galdar, which contribute but to a lesser extent (Figure 4.2).

This is why we can say that the municipalities of the southeast are the current lungs of wind energy production, as we can see in the figure 4.2, and also have a development towards the future for the implementation of more off-shore wind farms [10].

We have decided to choose the island of Gran Canaria to carry out the development due to all those mentioned conditions and also because the island has a large presence of wind farms before this study. This will help us to compare the results and, if our work is well underway, it will be also easier to use the present wind farm distributions as a model.

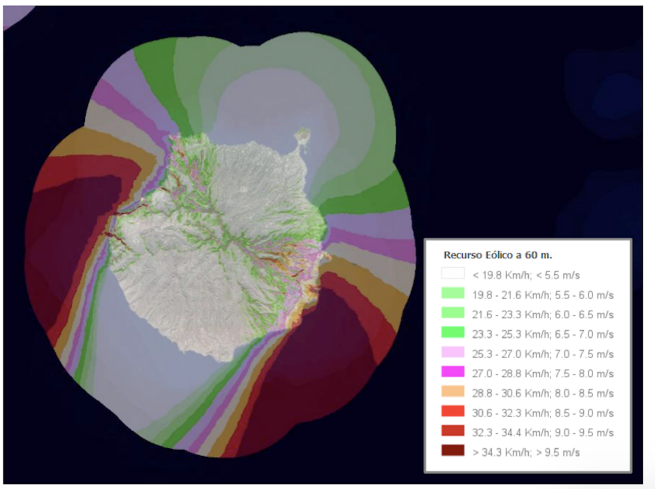

Figure 4.3: IDECanarias. Gran Canaria wind map

So, we know that the island presents adequate conditions for the implantation of farms, but as we commented before, the existence of protected natural areas in the surface of the island already presents zones where farms cannot be located due to their protection. We must also mention that these areas are joined by areas with populations or urban areas where it is not possible to establish farms either.

Finally, the question we ask ourselves is whether the remaining territory of the island can really be useful to achieve the necessary and sufficiently stable wind power in order to improve the current contribution of renewable energies.

4.2 Data

The data used in this study were taken from a previous work [11] in which the wind in the Canary region and its future evolution was simulated using the WRF mesoscale atmospheric model [12]. In that work, 10-year simulations were carried out, from which the one corresponding to the recent past, 1995-2004, was taken. The spatial resolution of the simulations was 5 km and the outputs had a temporal resolution of 2 hours. In addition to the wind speed, the extractable wind power was provided, calculated by considering a curve from a specific wind generator, the GAMESA-G97-2MW, with a hub height of 80 m. This curve is plotted in Figure 4.4.

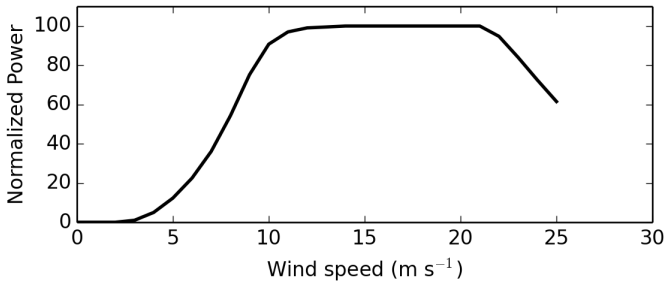

Figure 4.4: Power curve of a typical modern turbine (GAMESA-G97-2MW) normalized by the turbine nominal power.

4.3 Regionalization

4.3.1 The case of three regions

The first method we have used to carry out the study consists of dividing the island of Gran Canaria into three areas that are grouping pixels according to certain shared characteristics.

Firstly, we need to know what pixel (grid point of the physical simulations) will be a possible place to locate a wind farm. To do this, we have to discard all pixels that correspond to protected areas or high populated zones. Finally, after discarding these pixels, we can continue with the classification of the different zones.

In order to classify each zone we have made use of 4 different types of grouping methods, Spectral clustering, Mean Shift, Agglomerative clustering and Maximum PCA (Principal Component Analysis).

Figure 4.5: Results of the four clustering methods tested in this study.

Climatological data were provided in a netCDF file format. These files are characterized by storing data in multi-dimensions and the user can access each element of dimensions such as latitude, longitude, level, time.[13] The dataset contains dimensions, variables, and attributes, which all have both a name and an ID number by which they are identified.

In our case, the variables of interest are latitude, longitude, EWP (Extractable Energy Power) and time. The file collects a compilation of wind speeds in Gran Canaria by pixel taking the entire surface of the island. Although really as we commented in the previous section, the farms can not be implemented throughout the island, therefore before applying the methods of clustering it is necessary to know which pixels are intended for urban areas and which are protected areas.

To do this we generated two netCDF files, one of them for the areas declared as protected space and the other for the urban areas. With this, we created a mask to be able to mark these pixels as not available for the method. As a result, from the initial grid points 43 were finally obtained in which it would be possible, in principle, to place a wind farm.

Once we have this, we can proceed to apply the different clustering methods and choose the one that

suits us best. As we can see in the figure 4.5 and as we commented before, we tested four different methods and also, we can observe that despite being 4 different methods, the zones are characterized similarly to each other

Before applying the clustering algorithms, we are going to define the 4 different clustering that we calculated. The PCA technique was applied to the time series of the 43 grid points in order to reduce the initial features and facilitate clustering. Principal component analysis is a statistical technique for reducing the dimensionality of a dataset[15].

The first method is the Spectral Clustering that makes use of the spectrum (eigenvalues) of the similarity matrix of the data to perform dimensionality reduction before clustering in fewer dimensions[14]. The Mean Shift performs a non-parametric feature-space mathematical analysis technique for locating the maxima of a density function, a so-called mode-seeking algorithm[16].

The Maximum PCA, simply groups those pixels that have their highest value in the same principal component. The last one is the Agglomerative clustering, that is the one we are going to use. This type of clustering is the most common type of hierarchical clustering used to group objects in clusters based on their similarity [17]. It is represented as a tree (or dendrogram). The root of the tree is the unique cluster that gathers all the samples, the leaves being the clusters with only one sample [18].

Agglomerative Clustering is a bottom-up approach, initially, each data point is a cluster of its own, further pairs of clusters are merged as one moves up the hierarchy. The steps that the clustering follow are[19]:

1. Initially, all the data-points are a cluster of its own.
2. Take the two nearest clusters and join them to form one single cluster.
3. Proceed recursively step 2 until obtain the desired number of clusters.

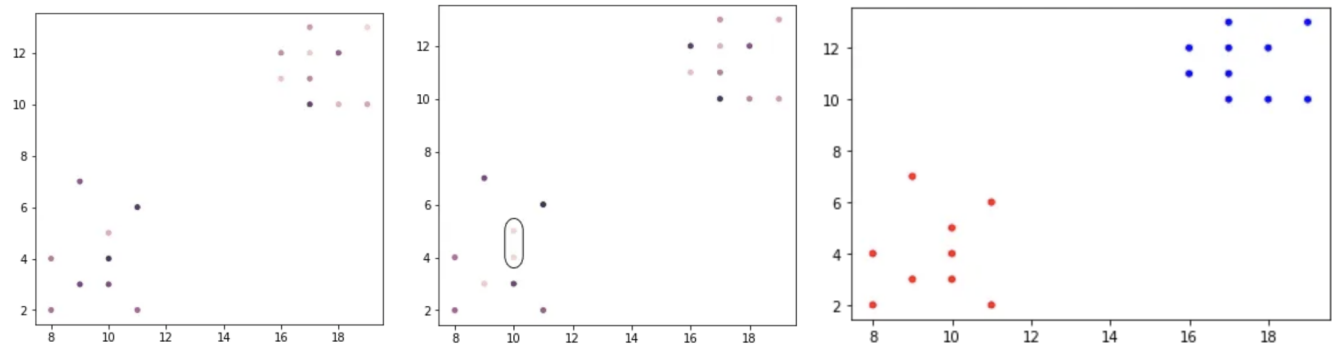

((a)) ((b)) ((c))

Figure 4.6: (Image by Satyam Kumar on Agglomerative Clustering and Dendrograms - Explained, Towards Data Science [19]) a) All the data point is a cluster of its own. b) the two nearest clusters (surrounded by a black oval) joins together to form a single cluster. c) the data separated into 2 clusters

Using the mentioned methods, we have obtained the three zones shown in Figure 4.5, except for the case of the Mean Shift algorithm. We have that for the Mean Shift, unlike the other methods, we cannot introduce the number of zones we want, i.e., the method itself makes a separation based on the data presented and when these values have a fairly low bandwidth it presents some meaningless groups. This explains the presence of a fourth zone in this method.

Finally, we will use the clustering obtained with the method Agglomerative, which produces areas more similar to what one might expect given the wind conditions on the island. We can see how the three zones are perfectly differentiated; zone zero is violet, zone one is the blue and the remaining zone is zone two. As we can see, zone zero, violet, is the one that contains more pixels and this is because the southeast and northwest wind have very similar temporal behaviour, we can see in the figure 4.3. We can also highlight that this zone coincides with the territories where there are currently more farms, see Figure 4.2, which supports the previous classification.

Next, we have looked to group the zones and their respective data. We created a program that, specifying the method, is able to recognise each pixel and to which zone it belongs, saving data in three different files, one for each zone. Finally, we worked with these files to obtain time series of the mean extractable power of each zone.

4.3.2 The case of 43 regions.

For this case, we have studied each pixel. We have omitted the clustering part, which means that now every pixel is an individual zone.

The total number of pixels in which the turbines can be placed is 43, which is the total number of pixels on the surface. As we did in the previous section, we have avoided the territories containing protected natural areas and those areas with a larger population and urban areas.

In conclusion, we have studied a more detailed distribution for the island of Gran Canaria.

5. OPTIMIZATION METHODOLOGY

Firstly, from the time series of the extractable wind power, the appropriate distribution of the wind farms will be analyzed, according to the desired objective, the maximization of the average generated power, the minimization of the variability of the production, or a compromise between both.

Starting by the case of the three regions, we will look for the percentage of installed power in each of them to achieve the indicated objectives. Subsequently, the distribution of wind farms among the 43 grid points discussed in the previous chapter will be analyzed.

For both cases, we resolved the Multi-objective Optimization using a genetic algorithm called NSGA-II. Finally, we had been capable to have a distribution of the positions of the wind turbine, in percentage, for the first case and the second one.

5.1 The case of three regions

As discussed in the previous chapter, we have identified three different wind climate regions (Figure 4.5.b), the first is the violet one (southeast, east and northwest), next is the blue(southwest) and lastly the yellow (northeast).

The optimization procedure requires a single time series of wind energy for each region. Therefore, for each of the three regions and for each time step, the power of all the corresponding pixels has been averaged, obtaining three time series with a resolution of 2 hours. Then, the wind energy time series, P_{ij}, have to be arranged according to a weighted averaging to obtain the corresponding time series for the whole island.

For instance, the time series of wind power for the whole island can be calculated as $\sum_j w_j P_{ij}$, where j indicates the region (j = 0, 1, 2), i corresponds to the time step and $\sum_j w_j = 1$. The value of weights w_j corresponds to the percentage of wind turbines in each of the zones 0, 1 and 2.

We had supposed that we place αN turbines in the zone 0, βN into the zone 1 and γN into the zone 2, where N is the total number of turbines, with $\alpha + \beta + \gamma = 1$. The time series of the overall power

output can be written as

$$P_i(\alpha,\beta,\gamma) = N(\alpha P_{i,0} + \beta P_{i,1} + \gamma P_{i,2}) \tag{5.1}$$

where $P_{i,0}$, $P_{i,1}$ and $P_{i,2}$ are the wind power time series for each of the three zones. Then the average power output can be computed as:

$$\langle P \rangle = \frac{\sum_i P_i}{n} \tag{5.2}$$

where n is the size of the time series. The mean variability has the form:

$$\langle \Delta P \rangle = \sqrt{\frac{\sum_i (P_i - P_{i-1})^2}{n}} \tag{5.3}$$

And to finish, the standard deviation:

$$\sigma = \sqrt{\frac{\sum_{i=1} \left(P_i - \langle P \rangle\right)^2}{n-1}} \tag{5.4}$$

The calculation is performed assuming different triplets in the space of the parameters $S = \{\alpha,\beta,\gamma \in \mathbb{R} : 0 \leq \alpha \leq 1; 0 \leq \beta \leq 1; 0 \leq \gamma \leq 1\}$

In Figure 6.1 the space of the α,β and γ parameters is represented, which range from 1 in the corresponding vertex to 0 on the opposite side along the medians: the condition $\alpha+\beta+\gamma = 1$ is then satisfied, as the sum of the distances from any point inside the figure.

The shaded contours represent the values of the three calculated variables $\langle \Delta P \rangle$, $\langle \Delta P \rangle$ and σ. The x label is α, the y-label is β and for γ we have, $\gamma = 1 - \alpha - \beta$.

We will discuss the results of these plots in the next chapter, now we are going to continue with the minimization of the function.

The concept known as Pareto Efficiency comes from the economics field. It is used to analyze an individual's possible optimal choices from a variety of objectives or desires and one or more evaluation criteria. Given a "universe" of alternatives, we seek to determine the Pareto efficient set (i.e., those alternatives that satisfy the condition of not being able to better satisfy one of those desires or objectives without worsening some other). That set of optimal alternatives establishes the Pareto Frontier. The study of the solutions in the frontier allows designers to analyze the possible alternatives within the established

parameters, without having to analyze the totality of possible solutions [20].

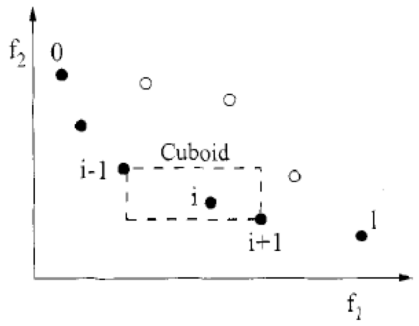

Figure 5.1: (Image by [23]) Pareto Front

Figure 5.1 depicts the concepts of Pareto optimality, thus allowing us to visualise how the Pareto optimal sets are defined and how the dominated and non-dominated solutions to the problem are identified.

In this work, we have used the Multi-objective Optimization Pymoo[21] module for Python, to find a solution using a Multi-Objective Optimization.

Without any loss of generality an optimization problem can be defined by:

$$\begin{array}{lll} \min & f_m(x) & m = 1,\ldots,M \\ \text{s.t.} & g_j(x) \leq 0 & j = 1,\ldots,J \\ & h_k(x) = 0 & k = 1,\ldots,K \\ & x_i^L \leq x_i \leq x_i^U & i = 1,\ldots,N \\ & x \in \Omega & \end{array} \tag{5.5}$$

Where x_i represents the i-th variable to be optimized, $x = (x_1, x_2, \ldots, x_N)$, x_i^L and x_i^U its lower and upper bounds, f_m the m-th objective function, g_j the $j-th$ inequality constraint and h_k the k-th equality constraint. The objective function(s) f are supposed to be minimized by satisfying all equality and inequality constraints. If a specific objective function must be maximized (max f_i), one can redefine the problem to minimize its negative value $(\min -f_i)$. [21].

We will say that a solution x^1 dominates another solution x^2 if they follow the next conditions:

1. The solution x^1 is not worse that x^2 in all objective

2. The solution x^1 is strictly better than x^2 in at least one objective.

If any of the conditions are violated, the solution x^1 does not dominate the solution x^2 [22].

Next we needed to define the algorithm we wanted to use. In our case we use NSGA-II(Non-Sorting Genetic Algorithm II), that present some characteristics that we can sum up in two point:

- Firstly, it establishes a quick mechanism for comparing solutions.
- Secondly, it establishes a measure of distance between solutions

Both points are ideal for the Pareto front. Continuing with NSGA-II this algorithm was proposed by Deb et al. [23]. Firstly a random parent population P_0 is created based on the non-domination. Every solution is assigned a fitness equal to its non-domination level((1 is the best level, 2 is the next-best level, and so on). At first, the usual binary tournament selection, recombination, and mutation operators are used to create an offspring population Q_0 of size N.

We first describe the Tth generation of the proposed algorithm as shown in the figure 5.2. Then, method start when a combined population $R_t = P_t \cup Q_t$ is formed. P_t and Q_t are two different populations that are going to combine. The population R_t is of size 2N, because each population have size N. Then, the population R_t is categorized according to non-domination. Since all previous and current population members are included in R_t, elitism is ensured.

Now, solutions belonging to the best non-dominate set F_1 are of best solutions in the combined population and must be emphasized more than any other solution in the combined population. If the size of F_1 is smaller than N, we definitely choose all members of the set for the new population P_{t+1}. Thus, the solutions from the set F_2 are chosen next, and the solution from the set F_3, and so on. In general, the count of solutions in all sets from F_1toF_l would be larger than the population size, where F_l is the last non-dominated set beyond which no other set can be accommodated.

The new population P_{t+1} of size N are chosen from subsequent non-dominated fronts in the order of their ranking. This procedure is continued until no more sets can be accommodated. As soon as the sorting procedure has found enough number of fronts to have N members in P_{t+1}, there is no reason to continue with the sorting procedure. Finally, the population P_{t+1} of size N will be used for selection, crossover, and mutation to create a new population Q_{t+1} of size N [23].

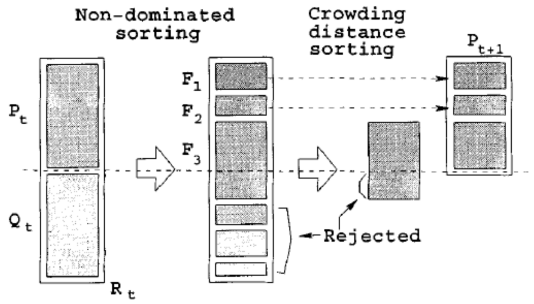

Figure 5.2: (Imagen by [23])NGSA-II diagram

So the functions we are going to maximise or minimise will be defined by:

$$\begin{aligned} \max . & f_1(x) = \langle P \rangle \\ \min . & f_2(x) = \langle \Delta P \rangle \\ \text{s.t. } & g_1(x) = x_1 + x_2 - 1 \\ & 0. \leq x_1 \leq 1. \\ & 0. \leq x_2 \leq 1. \\ & x \in \mathbb{R}^2 \end{aligned} \tag{5.6}$$

Where we can see that f_1 is 5.2, f_2 is 5.3. In this case, variability would be minimized and power would be maximized. It has also been tried to minimize the standard deviation, instead of the variability:

$$\begin{aligned} \max . & f_1'(x) = \langle P \rangle \\ \min . & f_2'(x) = \sigma \\ \text{s.t. } & g_1'(x) = x_1 + x_2 - 1 \\ & 0. \leq x_1 \leq 1. \\ & 0. \leq x_2 \leq 1. \\ & x \in \mathbb{R}^2 \end{aligned} \tag{5.7}$$

In this second case, we defined the functions f_1' as 5.2 and f_2' as 5.4.

Two different cases have been analyzed, one with Power and Variability and the other with Power and Standard Deviation. Also, we already said that if we want to maximize the function we need to redefine the problem to $(\min -f_i)$.

5.2 The case of 43 regions

A straightforward extension of the procedure shown in the previous section is the calculation of the $\langle P \rangle = max$ distribution, the $\langle \Delta P \rangle = min$ distribution and the $\sigma = min$ distribution for the 43 point of the grid that belong to the island and correspond to areas where wind turbines could be placed. As we said in the introduction of the chapter, now we will have x_i, where i $= 1, 2....43$, meaning that now the wind turbine will be located per pixel. The total power is described as:

$$P_i(\alpha_1, ..., \alpha_{43}) = N(\alpha_1 P_{i,1} + ... + \alpha_{43} P_{i,43}) \tag{5.8}$$

Where $\alpha_1 + \alpha_2 + ... + \alpha_{43} = 1$ represent the distribution of N turbines in each pixel of the island and $P_i(\alpha_1, ..., \alpha_{43}))$ is the wind power for the time step i. The mean total power output, $\langle P \rangle$, its variability, $\langle \Delta P \rangle$, and its standard deviation,σ , as a function of the parameters $(\alpha_1, ...\alpha_{43})$ are defined analogously to equations 5.2, 5.3 and 5.4, respectively.

Using the NSGA-II for Multi-Objective Optimization and specifying the same conditions we will get the results for the 43 pixels. Finally, with the alpha values obtained from the optimisation we have made a representation that will give us the distribution of wind turbines by percentages for each of the 43 available pixels.

6. RESULT AND DISCUSSION

6.1 The case of three regions

In this section, we present the results obtained using the methodology described above.

The maximum mean power distribution $\langle P \rangle = max$ is trivial. We can see in Figure 6.1(a) that it is located in the values $\alpha = 1, \beta = 0$ and $\gamma = 0$. This means the greater number of wind turbines should be placed in that area that corresponds with the zone 0 and where we previously commented the greater number of parks are already located.

For the variability (Figure 6.1(b)), we obtained that $\langle \Delta P \rangle = min$ at the point $\alpha = 64\%, \beta = 9\%$ and $\gamma = 27\%$. In this case, contrary to the maximum total power, the objective is to keep it as low as possible. The largest percentage of the turbines should be located in zone 0, although 36% would now be distributed among the other zones.

For the standard deviation (Figure 6.1(c)), we found that $\sigma = min$ at the point $\alpha = 32\%, \beta = 20\%$ and $\gamma = 48\%$. As for the variability, we are looking for the standard deviation to be as small as possible. We can see that the distribution is more focused in the zone 2, in contrast to the variability and power.

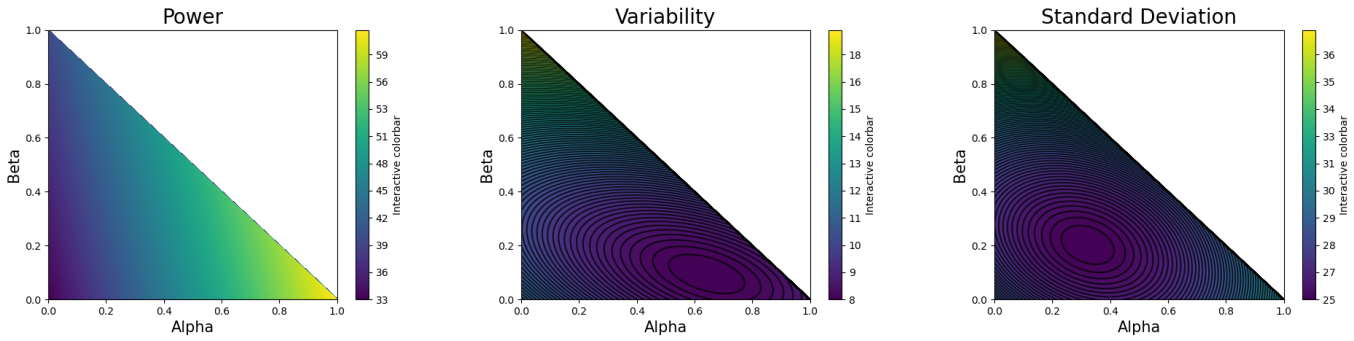

((a)) Power ((b)) Variability ((c)) Standard Deviation

Figure 6.1: At the left we have the power, at the center is the variability and at the right is the standard deviation

In the three cases studied the worst zone is the zone 1, if we observe the figure 4.5 this zone is the blue and it corresponds to the southwest of the island of Gran Canaria. Now, if we observe the figures 4.2 and 4.3 we can say that in this there zone exits a lack of wind resource and wind farms, so these results agree with the prior knowledge of the wind resource of the island.

For the variability and the power the best zone is the zone 0 that corresponds to the southeast and northwest and also is the zone that covers more surface, so that makes sense that this zone is so ideal for the distribution. Also, if we observe the figures 4.2 and 4.3 again, this zone has the highest percentage of wind farms of all the island, and as we said, this area is considered as the present lungs of wind energy. We can add that the dominant winds, named the Alisios, blow normally in North-East direction [25].

Why are these results not similar to those obtained for the standard deviation? To answer this question we need to focus on the definition of each magnitude. While variability measures the difference between one value and the next one, standard deviation gives us the difference with the average of all values. That is why we can say that the standard deviation is an atemporal magnitude.

Defining this, we can discuss why these results are different. For the variability we have that the zone 0 is where we can find the minimum, so this means that the highest concentration of wind farm are going to be there, and the rest in the order zones. For the standard deviation we have the same case, but now the minimum is achieved with the highest percentage of turbines placed in zone 2.

The Multi-Objective Optimisation results are summarized in the Pareto front, Figure 6.2, that gives us a very clear view of the results pattern. In this case, it shows us that we will never have the best conditions for the two magnitudes. That is, if we want $\langle P \rangle = max$ we will obtain $\langle \Delta P \rangle = max$. Pareto Front allows visualization of efficient options. A compromise must be reached between 'losing' a percentage of power to reduce system variability. Therefore we cannot have the optimal conditions for both magnitudes, as we said. The same happens with the standard deviation.

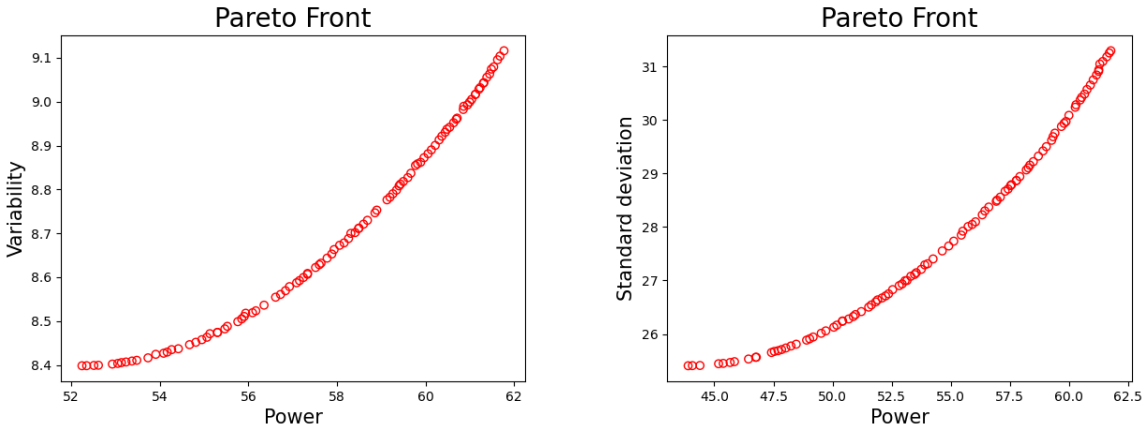

((a)) Variability / Power

((b)) Standard deviation / Power

Figure 6.2: Pareto Front

If we observe Tables 6.1 and 6.2 we can see the values for both endpoints of the curve. As we said in the previous paragraph, we will never have the perfect conditions for both values. In both cases, the maximum of power is normalized (to 100) and the distribution is the same that we have in 6.1(a). The same happens with the distribution for the variability and the standard deviation, which is the same that we got from the Figures 6.1(c) and 6.1(b).

	$\langle P \rangle$	$\langle \Delta P \rangle$	α	β	γ
Maximum Power	61,72	9,12	100%	0	0
Minimum Variability	52,24	8,40	64%	9%	27%
$0.95 \cdot \langle P \rangle_{\max}$	58,68	8,75	88%	5%	7%

Table 6.1: Result of the Power and Variability

	$\langle P \rangle$	σ	α	β	γ
Maximum Power	61,76	31,29	100%	0	0
Minimum Standard Deviation	43,89	25,40	32%	20%	48%
$0.95 \cdot \langle P \rangle_{\max}$	58,68	29,32	86%	12%	2%

Table 6.2: Result of the Power and Standard Deviation

To finish, we have calculated what will happen if we decided to sacrifice a percentage of the power, i.e, if we move out of the maximum power value. For the Variability, we can see in the Table 6.1 that

if we decide to obtain the 95% of the maximum power we will have a better value for the variability. Also, we can see how the distribution changes, the zone 0 remains the one with the highest wind farm percentage and then the zone 2 and the last is the zone 1. This case can be seen as a mix between the maximum and minimum values for the power and variability.

In Table 6.2 we can see that if we sacrifice the 5% of the maximum power we obtained a different distribution for the 3 regions. The α is the best zone, like the other cases, but if we observe β and γ we see the change. For this case the β presents the second highest distribution and the γ the last one. This can be seen as how we can change the distribution around the island if we decide to explore all the values that the Multi-Objective Optimisation gives us, and what happens if we decide to prioritize one value over the other.

6.2 The case of 43 regions

The result for this case is difficult to represent in a simple chart, so we have to go straight to the optimization computation. Just like the previous section, we had obtained the Pareto for each iteration number.

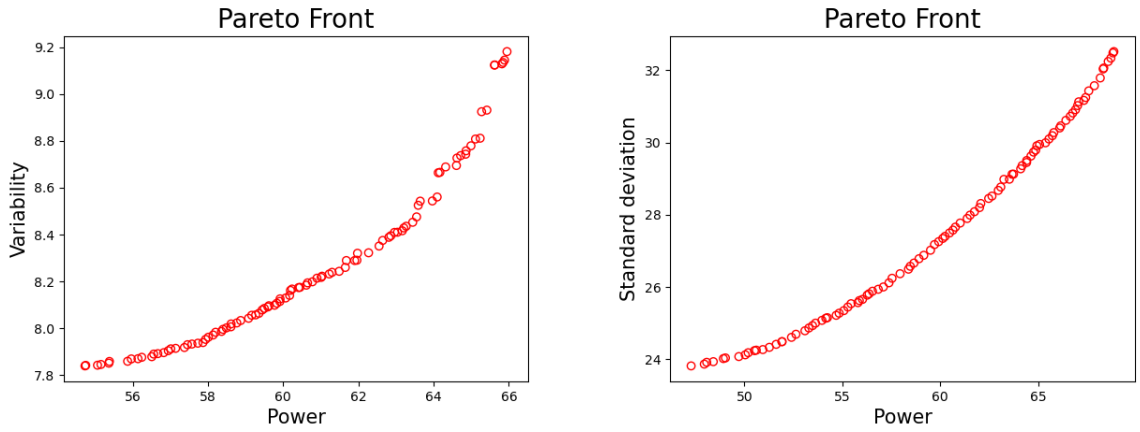

((a)) Variability / Power

((b)) Standard deviation / Power

Figure 6.3: Pareto Front for 200 iterations

The Pareto front from the solution run of the proposed NSGA-II can be observed in Figure 6.3. This result is for 200 iterations, and as we see we have obtained a well-formed Pareto front. We can emphasize that as the iterations rate increases, so does the convergence generation, which means longer simulation times, but greatly improves the optimal solutions.

	$\langle P \rangle$	$\langle \Delta P \rangle$
Maximum Power	65,95	9,18
Minimum Variability	54,72	7,83
$0.95 \cdot \langle P \rangle_{\max}$	62,65	8,37

Table 6.3: Result of the Power and Variability for 43 regions

	$\langle P \rangle$	σ
Maximum Power	68,86	32,51
Minimum Standard Deviation	52,72	23,82
$0.95 \cdot \langle P \rangle_{\max}$	65,42	29,99

Table 6.4: Result of the Power and Standard deviation for 43 regions

Tables 6.3 and 6.4 show the values for the power, variability and standard deviation in the case for the maximum and minimum.

Finally with the dominant solutions, the 43 percentages, one for each pixel, can be displayed on the map. As we can see in Figures 6.4 and 6.5, the distribution in the surface of the island is quite similar.

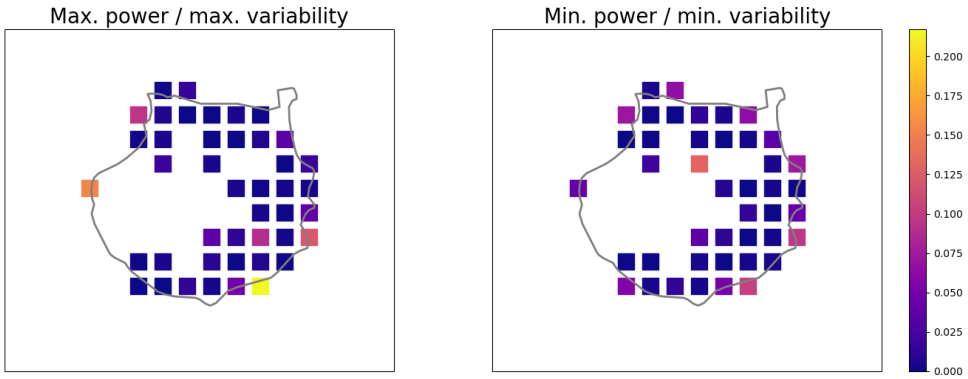

Figure 6.4: Power / Variability

Figure 6.4 is for the power and the variability. On the left we have the maximum for both magnitudes and we can see that there are three pixels that stand out more than the others. The one with the maximum value is in the southwest of the island and the two next are in the southwest and in the east. Compared

with Figure 4.2, the distribution is similar to the actual wind farm that the island presents. So, we can say that the island has a distribution based in obtaining the maximum power.

On the right of Figure 6.4 is the distribution for the minimum of the values. Here the distribution has a maximum in the municipality of Valleseco that is located in the North of the island, and the next values are more distributed around the island. The first anomaly is present here, because compared with the figure 4.2, in this zone of the island there is any wind farm.

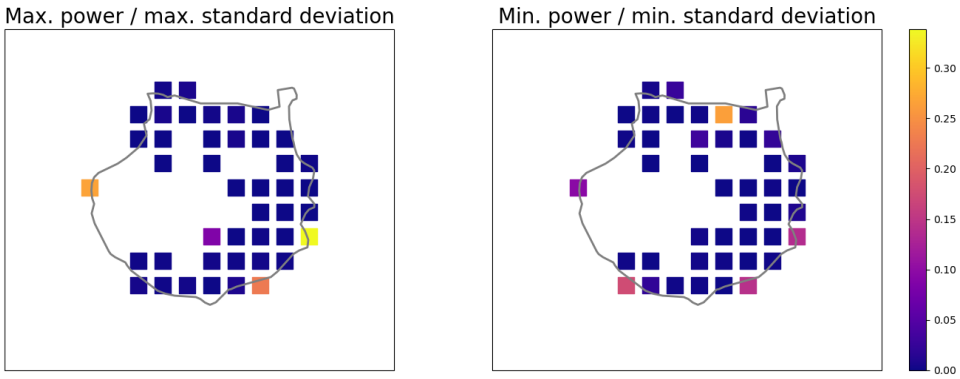

Figure 6.5: Standard Deviation / Power

Now for Figure 6.5 we have obtained another distribution. On the left is the maximum value for the standard deviation and for the power. As happened in the maximum case for Figure 6.4, the maximum value is in the southwest of the island and the next two more notable are in the southwest and east. On the right is the case for the minimum, where the highest percentage of wind farms is located in the north of the island, in the municipality of Arucas. The other pixels present a similar weight, with four that have a value over 10%.

Looking at both figures, 6.4 and 6.5, we can observe several similarities and differences. Principally, the distribution for both figures is considerably similar; for example, the maximum percentages are close to be in the same pixel. For the maximum power, the pixels with the highest number of wind turbines are in the municipality of San Mateo, Agüimes and San Bartolomé de Tirajana. This distribution is quite similar to the one in Figure 4.2. Something similar happened with the minimums figures. The pixel with the highest percentage is in the north, not in the same municipality but closer.

However, we can find some differences between both distributions. The most notable is that for Figure 6.5 the distribution is more located in 4 leading pixels and the rest of them are 5 percentual points lower than in Figure 6.4, where we can see that there are more pixels over 5%.

Furthermore, comparing the figures for both cases we can see that the pixels with the highest percentages are inside zone 0, which is also the zone with the highest percentage. For the minimum variability and standard deviation, the percentage is more distributed as in the three case regions. So we can agree that both cases present a similar distribution.

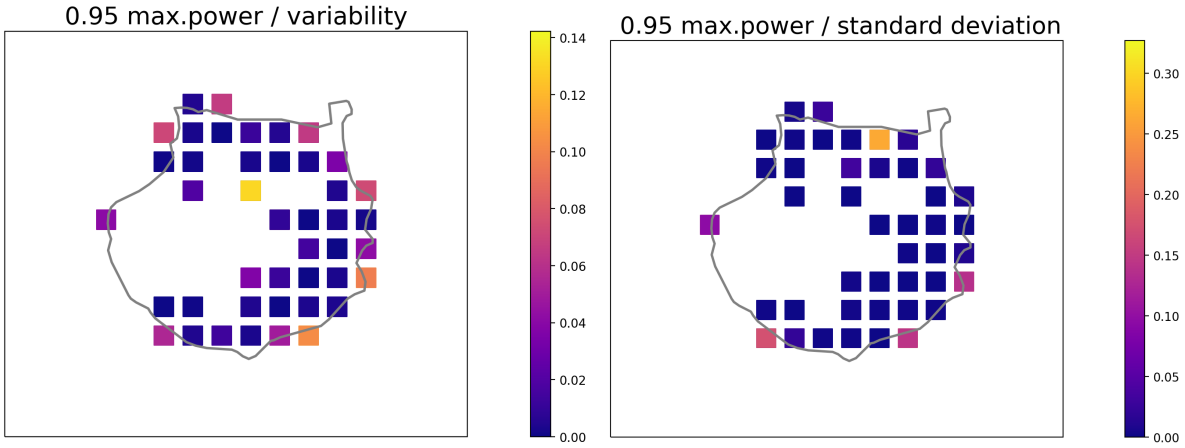

((a)) Variability / Power

((b)) Standard deviation / Power

Figure 6.6: Distribution for the $0.95 \cdot \langle P \rangle_{\max}$

In Figure 6.6 we can observe two maps that correspond with the distribution of the 95% of the maximum power.

Figure 6.6(a) corresponds to the case of the variability. Now if we compare this with the distribution in Figure 6.4 we can see that sacrificing a 5% of the maximum power allows us to have a new distribution that is like a mixture of these two previous distributions. In the new distribution we can appreciate that the new maximum moves to the north of the island and the other two highest points of distribution stay in the southeast of the island. Also we can observe that the maximum percentage of distribution has decreased, so now the pixel with the highest percentage is only 14%.

For Figure 6.6(b) we can observe the case for the standard deviation. In this distribution, the maximum is, again, in the north of the island and the next pixels are in the southeast/southwest of the island. Comparing it with the distribution in Figure 6.5 we can see that we obtain a mix of both cases as happened with Figure 6.6(a). But now, this new distribution looks more like the case for Min. power and standard deviation, i.e.,

when we reduce a 5% the maximum power, we obtain a distribution that has a lower standard deviation.

So, for the cases in Figure 6.6 we slightly reduce the power and at the same time, we obtain an improvement value for the variability or the standard deviation.

As we see in the previous cases, sometimes the wind turbines would be very dispersed. One possibility would be to establish a criteria for a minimum and maximum percentage of wind turbines that can be placed in each pixel. As an example, two new conditions have been added to the previous optimizations. In each of the zones occupied by wind farms, a minimum of 10% of the production must be accounted for, and none of these zones can accumulate more than 30%. The corresponding Pareto front is shown in Figure 6.7. In this case, the power has been maximized and the standard deviation has been minimized. The distribution of wind turbines, as a percentage, is shown in Figure 6.8. Compared to the previous results, we can see that the percentages are higher, concentrating the placement of the turbines in very few areas.

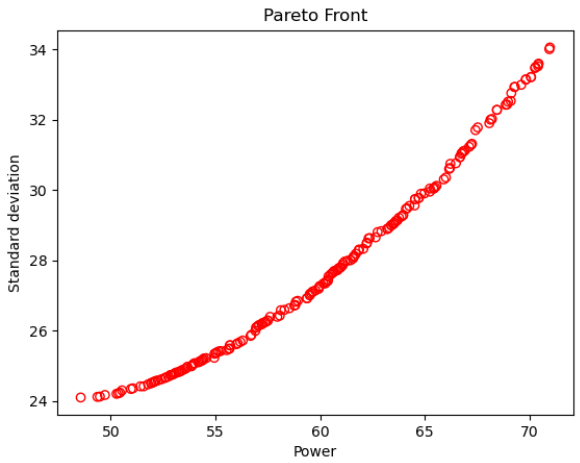

Figure 6.7: Pareto front for the opmisation with minimum and maximum percentages restrictions.

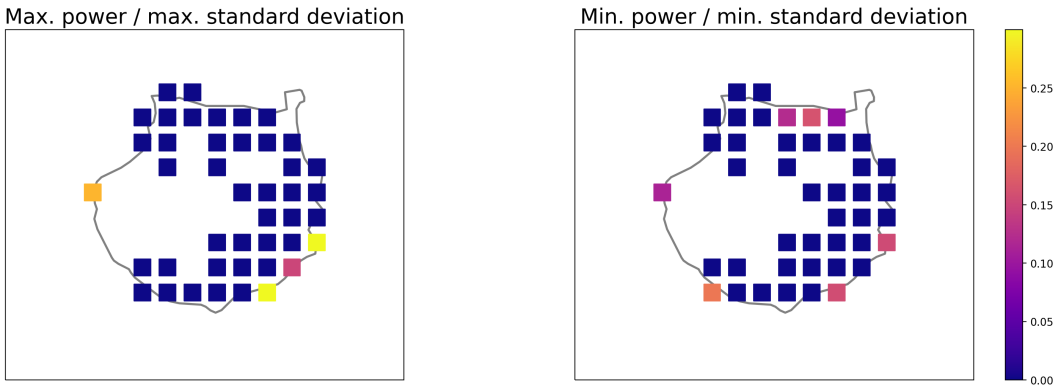

Figure 6.8: Results for the opmisation with minimum and maximum percentages restrictions.

For the case in which the power is maximized, the selected zones are again the same in which the wind is stronger, and even a slightly higher average normalized power, 71.0, is obtained, compared to the one shown in the Table 6.4 However, at the other extreme, when the deviation is minimum, the value remains very similar to the results shown in that table, 23.95, but with a lower average power output, 48.5.

7. CONCLUSIONS

In the present study, we have proposed a procedure to calculate the optimal distribution of wind farms over a territory by the optimisation of different magnitudes.

In order to do so, our methodology consisted on using a dataset from wind simulations from 2007 to 2005 to create a model of how the new wind energy projects to be implemented on the island should be optimally located. This method presents the novelty that it does not classify a single space as the optimal, but it makes a distribution in percentages over the whole territory that assure a more stable production of wind energy throughout the year. Furthermore it allows us to decide what percentage of power to give up in order to minimize system variance.

We have tested the method over Gran Canaria, the third largest island in the Canarian Archipelago. Firstly we divided the region of study into three zones using a cluster analysis based on the wind data of the territory, where the spatial distributions of wind farms was calculated considering three parameters only. Then, a straightforward extension was applied to extend the calculation of such distributions to 43 regions that correspond to the total available territory of the island.

The solution that we obtained , using a Multi-objective optimization and the NSGA-II algorithm, presents a great similarity with the already existing distribution in the island, leading to the conclusion that the current distribution is based on obtaining the maximum power over other magnitudes, such as variability or the standard deviation.

Moreover, it should be noted that this distribution not only presents a benefit for the production of less variable energy, but it also presents a distribution plan that avoids the creation of hyper-accumulation areas of farms along the island and that it is ultimately a kind of contamination of the natural landscape of certain areas.

However, current electric distribution infrastructures have not been taken into account in this work, so their inclusion could be another restriction to the overall problem. In addition, the standard deviation has been directly calculated on the normalized time series of extractable power, in order to take also into account seasonal variations. Alternatively, the deviation on hourly anomalies could be studied, in

order to further weigh the higher frequency oscillations of the production. These improvements could be addressed in future works.

Furthermore, this study suggests an investment towards more structures linked to green energies making a lot of environmental benefits, as CO2 emission reduction. As well as providing a new framework for future research, because as we have obtained the distribution for the island, future studies can use the same methods for off-shore distribution around the island.

To sum up, the wind power in the islands presents an important resource to obtain energy without any emission and, with this study, we have calculated how future distributions can have a more effective production of energy.

BIBLIOGRAPHY

[1] Rosario J. Marrero, Juan Andrés Hernández-Cabrera, Ascensión Fumero and Bernardo Hernández **Social Acceptance of Gas, Wind, and Solar Energies in the Canary Islands**, Universidad de La Laguna

[2] S.C. Pryor, R.J. Barthelmie **Climate change impacts on wind energy: A review**, 2010

[3] GORONA DEL VIENTO S.A, https://www.goronadelviento.es

[4] Red eléctica de españa **Avance del informe del sistema eléctrico español** , 2021

[5] Gran Canaria, https://en.wikipedia.org/wiki/Gran_Canaria

[6] Gran Canaria - Entre Montañas, https://entremontanas.com/islas-atlanticas/gran-canaria

[7] José Antonio Valbuena Alonso, Anuario Estadístico de la Energía en Canarias http://www.gobiernodecanarias.org/istac/jaxi-istac/menu.do?uripub=urn:uuid:131cf873-66a9-408d-8cfa-537d6be05067

[8] NSGA-II: Non-dominated Sorting Genetic Algorithm, january 2004 https://pymoo.org/algorithms/moo/nsga2.html

[9] Mostafa Abouei Ardakan, Mohammad Taghi Rezvan, **Multi-objective optimization of reliability–redundancy allocation problem with cold-standby strategy using NSGA-II** , Reliability Engineering and System Safety, 20018

[10] Pablo Sahuquillo Gabaldón, **Diseño y análisis de viabilidad económica de una instalación eólica offshore de 50MW ubicada en la costa de Gran Canaria** Universidad de Valencia (2022)

[11] A. González, J. C. Pérez, J. P. Díaz, F. J. Expósito, **Future projections of wind resource in a mountainous archipelago, Canary Islands**, Renewable Energy 104 (2017) 120 – 128. doi:10.1016/j.renene.2016.12.021.

[12] W. C. Skamarock, J. B. Klemp, J. Dudhia, D. O. Gill, M. Barker, K. G. Duda, X. Y. Huang, W. Wang, J. G. Powers, **A description of the Advanced Research WRF Version 3**, Tech. rep., National Center for Atmospheric Research (2008).

[13] What is an NC file (NetCDF) ? https://agrimetsoft.com/Default

[14] Spectral clustering, https://en.wikipedia.org/wiki/Spectral_clustering

[15] Principal component analysis, https://en.wikipedia.org/wiki/Principal_component_analysis

[16] Wikipedia, Mean Shift, https://en.wikipedia.org/wiki/Mean_shift

[17] Alboukadel Kassambara, Agglomerative Hierachical Clustering, 2019,https://www.datanovia.com/en/lessons/agglomerative-hierarchical-clustering/

[18] Scikits Learn 4.2 Clustering, https://scikit-learn.sourceforge.net/0.8/modules/clustering.html

[19] Satyam Kumar, Agglomerative Clustering and Dendrograms, 3 August 2020, https://towardsdatascience.com/agglomerative-clustering-and-dendrograms-explained-29fc12b85f23

[20] Pareto Efficiency, https://en.wikipedia.org/wiki/Pareto_efficiency

[21] Pymoo: Multi-Objetive Optimization in Python, January 2004, https://pymoo.org/index.html

[22] Carlos Adrían Correa Flórez, Ricardo Andrés Bolaños, Alexánder Molina Cabrerra, **Algoritmo multiobjetico NSGA-II aplicado al problema de la mochila**, Septiembre 2008

[23] Kalyanmoy Deb, Associate Member, IEEE, Amrit Pratap, Sameer Agarwal, and T. Meyarivan, **A Fast and Elitist Multiobjective Genetic Algorithm: NSGA-II** ieee transactions on evolutinary computation, Vol. 6, No. 2, April 2002

[24] FEDERICO CASSOLA, MASSIMILIANO BURLANDO, MARTE ANTONELLI, AND CORRADO F. RATTO, **OPTIMIZATION OF THE REGIONAL SPATIAL DISTRIBUTION OF WIND POWER PLANTS TO MINIMIZE THE VARIABILITY OF WIND ENERGY INPUT INTO POWER SUPPLY SYSTEMS**, 2008

[25] P. I. GONZÁLEZ DOMÍNGUEZ, G. HERNÁNDEZ LEZCANO, M. MARTÍNEZ MELGAREJO, A. PULIDO ALONSO, N. ANGULO RODRÍGUEZ, J. C. QUINTANA SUÁREZ, J. ROMERO MAYORAL **SENSIBILITY ANALYSIS IN THE STUDY OF ECONOMIC VIABILITY OF A WIND FARM IN THE CANARY ISLAND. A CASE OF STUDY: 10 MW WIND FARM IN ROQUE PRIETO, GÁLDAR, GRAN CANARIA.**, RE&PQJ, VOL. 1, NO.5, MARCH 2007

[26] STANDARD DEVIATION, 18 FEBRUARY 2023, HTTPS://EN.WIKIPEDIA.ORG/WIKI/STANDARD_DEVIATION

[27] GEORGE CARALIS, YIANNIS PERIVOLARIS, KONSTANTINOS RADOS AND ARTHOUROS ZERVOS, **ON THE EFFECT OF SPATIAL DISPERSION OF WIND POWER PLANTS ON THE WIND ENERGY CAPACITY CREDIT IN GREECE**, ENVIRON. RES. LETT. 3, 2008

[28] M.R. MILLIGAN AND R. ARTIG **CHOOSING WIND POWER PLANT LOCATIONS AND SIZES BASED ON ELECTRIC RELIABILITY MEASURES USING MULTIPLE-YEAR WIND SPEED MEASUREMENTS** JULY, 1999

[29] RAIK BECKER AND DANIELA THRÄN, **OPTIMAL SITING OF WIND FARMS IN WIND ENERGY DOMINATED POWER SYSTEMS**, ENERGIES, 2018

[30] TOMÁS GUOZDEN, JUAN PABLO CARBAJAL, EMILIO BIANCHI AND ANDRÉS SOLARTE **OPTIMIZED BALANCE BETWEEN ELECTRICITY LOAD AND WIND-SOLAR ENERGY PRODUCTION**, FRONTIERS IN ENERGY RESEARCH, VOL 8, ARTICLE 16, FEBRUARY 2020

[31] FRANCISCO SANTANA-SARMIENTO, FRANCISCA ROSA ÁLAMO-VERA AND PETRA DE SAÁ-PÉREZ **A RESOURCE-BAES VIEW OF COMPETITIVENESS IN THHE WIND ENERGY SECTOR: THE CASE OF GRAN CANARIA AND TENERIFE**, APPL. SCI. 2019

[32] KAOSHAN DAI, ANTHONY BERGOT, CHAO LIANG, WEI-NING XIANG, ZHENHUA HUANG **ENVIRONMENTAL ISSUES ASSOCIATED WITH WIND ENERGY E A REVIEW** , RENEWABLE ENERGY,2015

[33] CHRISTOPHER JUNG, DIANA TAUBERT AND DIRK SCHINDLER, **THE TEMPORAL VARIABILITY OF GLOBAL WIND ENERGY – LONG-TERM TRENDS AND INTER- ANNUAL VARIABILITY**, ENERGY CONVERSION AND MANAGEMENT, 2019

[34] SCOTT GREENE, MARK MORRISSEY AND SARA E. JOHNSON, **WIND CLIMATOLOGY, CLIMATE CHANGE, AND WIND ENERGY**, GEOGRAPHY COMPASS, 2010

[35] YUCHEN YANG, KAVAN JAVANROODI AND VAHID M. NIK, **CLIMATE CHANGE AND RENEWABLE ENERGY GENERATION IN EUROPE—LONG-TERM IMPACT ASSESSMENT ON SOLAR AND WIND ENERGY USING HIGH-RESOLUTION FUTURE CLIMATE DATA AND CONSIDERING CLIMATE UNCERTAINTIES**, ENERGIES, 2022

[36] S.C. PRYOR, R.J. BARTHELMIE, **CLIMATE CHANGE IMPACTS ON WIND ENERGY: A REVIEW** , RENEWABLE AND SUSTAINABLE ENERGY REVIEWS, 2010

[37] CARLOS A. GARCÍA, EDWIN GARCÍA Y FERNANDO VILLAD, **IMPLEMENTACIÓN DEL ALGORITMO EVOLUTIVO MULTI-OBJETIVO DE FRENTE DE PARETO (SPEA) PARA LA PLANEACIÓN DE SISTEMAS ELÉCTRICOS DE DISTRIBUCIÓN INCLUYENDO HUECOS DE VOLTAJE** , INFORMACIÓN TECNOLÓGICA, VOL. 26 NO 5, 2015